The Effect of Removing the N-Terminal Extension of the *Drosophila* Myosin Regulatory Light Chain upon Flight Ability and the Contractile Dynamics of Indirect Flight Muscle

Jeffrey R. Moore,* Michael H. Dickinson,† Jim O. Vigoreaux,‡ and David W. Maughan*

*Department of Molecular Physiology and Biophysics and ‡Department of Biology, University of Vermont, Burlington, Vermont 05405, and †Department of Integrative Biology, University of California, Berkeley, California 94720 USA

ABSTRACT   The *Drosophila* myosin regulatory light chain (DMLC2) is homologous to MLC2s of vertebrate organisms, except for the presence of a unique 46-amino acid N-terminal extension. To study the role of the DMLC2 N-terminal extension in *Drosophila* flight muscle, we constructed a truncated form of the *Dmlc2* gene lacking amino acids 2–46 (*Dmlc2*$^{\Delta2-46}$). The mutant gene was expressed in vivo, with no wild-type *Dmlc2* gene expression, via P-element-mediated germline transformation. Expression of the truncated DMLC2 rescues the recessive lethality and dominant flightless phenotype of the *Dmlc2* null, with no discernible effect on indirect flight muscle (IFM) sarcomere assembly. Homozygous *Dmlc2*$^{\Delta2-46}$ flies have reduced IFM dynamic stiffness and elastic modulus at the frequency of maximum power output. The viscous modulus, a measure of the fly's ability to perform oscillatory work, was not significantly affected in *Dmlc2*$^{\Delta2-46}$ IFM. In vivo flight performance measurements of *Dmlc2*$^{\Delta2-46}$ flies using a visual closed-loop flight arena show deficits in maximum metabolic power ($P^*_{CO_2}$), mechanical power (P^*_{mech}), and flight force. However, mutant flies were capable of generating flight force levels comparable to body weight, thus enabling them to fly, albeit with diminished performance. The reduction in elastic modulus in *Dmlc2*$^{\Delta2-46}$ skinned fibers is consistent with the N-terminal extension being a link between the thick and thin filaments that is parallel to the cross-bridges. Removal of this parallel link causes an unfavorable shift in the resonant properties of the flight system, thus leading to attenuated flight performance.

INTRODUCTION

Myosin, the molecule that interacts with actin to produce force and movement, consists of two heavy chains (~220 kDa) and four light chains (~20 kDa). The myosin light chains (MLCs) can be divided into two subclasses: the regulatory (MLC2) and essential (MLC1 and MLC3) light chains.

The *Drosophila* MLC2 (DMLC2) is encoded by a single gene located in region 99E1–3 on the right arm of chromosome 3 (Parker et al., 1985; Toffenetti et al., 1987). DMLC2 is homologous to MLC2s found in vertebrates (Parker et al., 1985). However, comparison of the MLC kinase substrate sites shows that the primary sites of phosphorylation in smooth muscle and skeletal muscle MLC2 (residues 19 and 12, respectively) correspond to residue 66 of DMLC2. The shift in MLC kinase (MLCK) substrate site in DMLC2 is due to a unique 46-amino acid N-terminal extension characterized by a stretch of basic amino acids at the N-terminus and a proline-alanine-rich sequence similar to the extension of MLC1 found in vertebrates (Fig. 1). The N-terminus of the MLC1 extension has been shown to interact with the actin region between Trp[355] and Cys[377] (Sutoh, 1982; Trayer et al., 1987). Rabbit myosin S1 exhibits a reduced detachment rate when assayed in vitro with *Drosophila*

actin containing a point mutation in this region that converts Gly[368] to glutamate (Anson et al., 1995). The reduced motility and detachment rate were interpreted as an altered contact between MLC1 of rabbit S1 with the mutant *Drosophila* actin (Anson et al., 1995). Curiously, flies expressing this mutant actin have reduced flight ability and a decreased rate constant of stretch activation (Drummond et al., 1990). In *Drosophila*, the essential light chain lacks the N-terminal extension found in rabbit MLC1. The N-terminal extension of DMLC2 has a sequence similar to that of MLC1 and therefore could explain the in vivo effects of the actin mutation.

The results obtained from flies expressing the C-terminal actin mutation suggest that the N-terminal extension of DMLC2 interacts with the thin filament, an interaction that may be required for the proper functioning of IFM. To address the role of the DMLC2 N-terminus, we used a molecular genetic approach to produce a truncated DMLC2 protein (DMLC2$^{\Delta2-46}$) that resembles MLC2 of vertebrates (Fig. 1). *Dmlc2*$^{\Delta2-46}$ flies, in which only DMLC2$^{\Delta2-46}$ is expressed with no endogenous DMLC2, were assayed for flight ability and wing beat frequency. The dynamic stiffness and mechanical power output of IFM isolated from mutant flies was also measured. The results show that removal of the N-terminal extension of DMLC2 has surprisingly little effect on the ultrastructure, mechanical properties, and in vivo function of IFM. However, *Dmlc2*$^{\Delta2-46}$ flies exhibit an altered behavior at the onset of flight. The slight reduction in maximum flight system power output, as measured from wing beat kinematic and metabolic measurements, may be due to a reduced dynamic stiffness of the IFM.
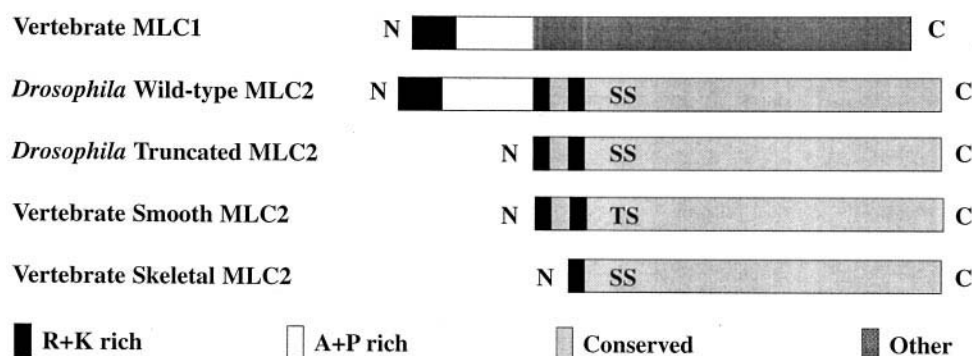
FIGURE 1 Schematic representation comparing the DMLC2 sequences to MLC2 sequences of vertebrate muscles. We constructed a truncated *Dmlc2*, *Dmlc2*$^{\Delta 2-46}$, where amino acids 2–46 were removed. Note that removal of the residues, which include the proline-alanine rich N-terminus, results in a DMLC2 protein that resembles MLC2s of vertebrate smooth and skeletal muscle. S and T indicate the MLCK substrate sites.

MATERIALS AND METHODS

Construction and transformation of the mutant DMLC2

The truncation of *Dmlc2*$^+$ involved the use of pCasJW1 (Warmke et al., 1992). pCasJW1 was constructed by Warmke et al. (1992) by inserting a 3.4-kb *Eco*RI/*Hind*III genomic DNA fragment, which contains the transcription unit as well as ~700 bp of 5′ flanking sequences and ~650 bp of 3′ flanking sequences, into the P-element transformation vector pCasPeR (Pirrotta, 1988). This vector has been used to rescue the *Dmlc2* null in a previous study (Warmke et al., 1992), thus demonstrating that it has the necessary sequences for proper expression.

To truncate the *Dmlc2*$^+$ gene a new restriction site (*Nco*I) was created by site-directed mutagenesis. A 436-bp *Pst*I-*Bam*HI fragment containing the end of intron 1 and about half of exon 2 from *Dmlc2*$^+$ was cloned into the single-stranded phagemid pAlter (Stratagene) for the generation of a single-stranded template. A mutagenic oligonucleotide containing the *Nco*I site was annealed at the 3′ end of intron 1 for the synthesis of the mutagenic strand. An ampicillin resistance repair oligonucleotide was also annealed to allow selection of mutants. Mutants were analyzed by restriction enzyme digest to confirm the incorporation of the mutagenic restriction enzyme site. Confirmed mutants were subcloned into the genomic *Dmlc2*$^+$ sequence and digested with *Nco*I and *Bst*BI. The DNA was treated with mungbean nuclease to create blunt ends and recircularized. This procedure restored the reading frame, as confirmed by DNA sequence analysis, and the resulting gene lacks codons for amino acids 2–46. After sequencing, the mutated *Dmlc2*$^+$ cassette was subcloned into the *Eco*RI and *Bam*HI sites of pCasJW1 for transformation. Transformation into host yw^{118} embryos was performed under standard conditions (Rubin and Spradling, 1982). The chromosome containing the transformed gene was introduced into a host strain lacking wild-type *Dmlc2* (*Dmlc2*^{E38}; Warmke et al., 1992) by standard genetic crosses. The resulting fly stocks expressed two copies of the mutant *Dmlc2* gene (*Dmlc2*$^{\Delta 2-46}$) and no functional copies of the wild-type *Dmlc2* gene (*Dmlc2*$^+$). Nine independent chromosomal insertions were created. Two lines mapped to chromosome 2 and one line mapped to the X. The rest of the lines mapped to chromosome 3 and have not been characterized further. We investigated one line on chromosome 2 and one line on the X chromosome in this study. The flight abilities of the two groups were indistinguishable ($p = 0.1$), and the results for flight index, wing beat frequency, and skinned fiber mechanics were pooled.

Electron microscopy

Thoraces were isolated from 2–4-day-old adult flies by dissection in fixation buffer containing 3% glutaraldehyde, 100 mM sucrose, 100 mM sodium phosphate buffer (pH 7.1), and 1 mM EGTA. The head and abdomen were removed with forceps. The dorsal longitudinal muscles were exposed by slicing the thorax in the midsaggital plane with a sharpened tungsten wire probe. The thoraces were then washed three times in Millonig's buffer for 5 min each and postfixed in OsO$_4$ for 30 min at 4°C, followed by three more washes with Millonig's buffer. Samples were then dehydrated with an ethanol series followed by propylene glycol and embedded in Spurr's resin.

Flight tests, wing beat kinematic, and metabolic measurements

The flight ability of individual flies was determined using a Plexiglas flight box (Drummond et al., 1990). Flies were released from their culture vials into the center of a Plexiglas box while a phototactic stimulus was presented from above. Flies with normal flight ability fly toward the light source, while flight-impaired mutants do not. Flies were scored as previously described (Tohtong et al., 1995).

After the assessment of flight ability, one of the fly's legs was tethered and the wing beat frequency was determined with an optical tachometer (Hyatt and Maughan, 1994).

To more thoroughly assess the in vivo consequences of truncating the DMLC2 protein, we examined the flight performance of mutant flies in a visual feedback closed-loop flight arena. The design of the flight arena, the means of tethering flies, and the methods for analyzing the resulting data have been described elsewhere (Lehmann and Dickinson, 1997; Dickinson et al., 1997). Briefly, the animals were placed within a cylindrical array of 1584 closed-packed LEDs that generate visual patterns that rotate around the tethered flying animal. The instantaneous wing beat frequency, stroke amplitude, flight force, and CO$_2$ flux were measured using a variety of dedicated optical sensors. The experiments were performed under closed-loop conditions, such that each fly controlled the angular velocity of a vertical 30° dark stripe by adjusting the stroke amplitude of its wings. Under such conditions, flies actively fixated the stripe in the front portion of their visual field. To assess maximum flight performance, we oscillated a superimposed pattern of horizontal stripes. Flies responded to upward motion of the horizontal stripe by increasing their total flight force output. Our measurements of wing beat amplitude, stroke frequency, and mass specific metabolic rate ($P^*_{CO_2}$) were pooled from all data within each 5–20-min flight sequence for those sequences in which force production was within 1% of its maximum value for the entire sequence. After each experiment, the animals were weighed and subjected to an array of anatomical measurements that permit calculation of mechanical power based on kinematics and morphology (Dickinson and Lighton, 1995; Lehmann and Dickinson, 1997). In total we compared six measurements of maximum flight performance: force to body weight ratio, wing beat amplitude,

stroke frequency, total metabolic rate ($P^*_{CO_2}$), mechanical power (P^*_{mech}), and mechanical efficiency, defined as the ratio of mechanical power to total metabolic power. The values were compared to those of Canton-S wild type made under similar conditions.

Skinned fiber mechanics

The skinned fiber mechanics of dorsal longitudinal muscle fibers was assessed as previously described (Dickinson et al., 1997). During and after dissection, the fibers were skinned in a relaxing solution (5 mM ATP, 15 mM creatine phosphate, 240 U/ml creatine phosphokinase (Sigma), 1 mM free Mg^{2+}, 5 mM EGTA, 20 mM *N,N*-bis(2-hydroxyethyl)-2-aminoethane sulfonic acid (pH 7.0), at an ionic strength of 175 mM adjusted with Na methane sulfonate) with 0.5% Triton X-100 for 1 h at 4°C. After skinning and mounting, the temperature was raised to 12°C and fibers were activated incrementally by exchanging equal volumes of activating solution (pCa 4.5) for relaxing solution up to pCa 5. Sinusoidal length changes were applied (0.25% of muscle length; peak to peak) over 47 frequencies from 0.5 to 1000 Hz. At each frequency, the tension and length signals were measured to obtain the fiber's complex stiffness modulus ($Y(f)$). The complex stiffness modulus is defined as the ratio of stress to strain in the frequency domain, where stress is the force per cross-sectional area and strain is the fractional length change ($Y(f) = \Delta F/A/\Delta L/Lo$). The frequency response function of a latex strip was used to correct for system characteristics.

RESULTS

Truncation reduces the number of DMLC2 phosphovariants

To determine the role of the DMLC2 N-terminus, a mutant gene ($Dmlc2^{\Delta 2-46}$) was created that encodes a DMLC2 in which the first 46 amino acids were removed. The resulting protein resembles vertebrate smooth muscle MLC2 (Fig. 1). The mutant gene was introduced into the *Dmlc2* null ($Dmlc2^{E38}$) background (Warmke et al., 1992) via P-element mediated germline transformation and standard genetic crosses. Flies homozygous for the transformed gene are referred to here as $Dmlc2^{\Delta 2-46}$.

DMLC2 has a calculated molecular mass of ~24 kDa. However, in sodium dodecyl sulfate-polyacrylamide gel electrophoresis (SDS-PAGE) wild-type DMLC2 migrates more slowly than expected as two bands between 30 and 33 kDa (Fig. 2, *A* and *B*). The reduced mobility suggests a tertiary structure that retards mobility during electrophoresis. Proteins extracted from $Dmlc2^{\Delta 2-46}$ flies show that the truncated DMLC2 migrates at its calculated molecular mass (Fig. 2 *A*).

Analysis of thoracic proteins by 2D SDS-PAGE (Fig. 2 *B*) reveals numerous isoforms of DMLC2 that result from phosphorylation (Takano-Ohmuro et al., 1990) (Fig. 2). Earlier studies designated these isoelectric variants as spots 138, 148, and 149 (Mogami et al., 1982). Higher resolution 2D gels demonstrate that each major spot defined by Mogami et al. (1982) consists of multiple isoelectric variants each for a total of ~14 (Dickinson et al., 1997). N1 and P1a through P1f correspond to spot 148, and P2a through P2g correspond to spots 138 and 149. N refers to nonphosphorylated and P refers to phosphorylated isoforms (Dickinson et al., 1997). A polyclonal antibody raised against a bacterially expressed DMLC2 confirmed the presence of ~14 antigenically related isoelectric variants, all of which except the most basic are phosphorylated (Fig. 2 *B*; see also Dickinson et al., 1997). These 13 variants can be divided into two molecular mass categories that correspond to the 30-kDa and 33-kDa bands of 1D SDS-PAGE (Fig. 2 *A*).
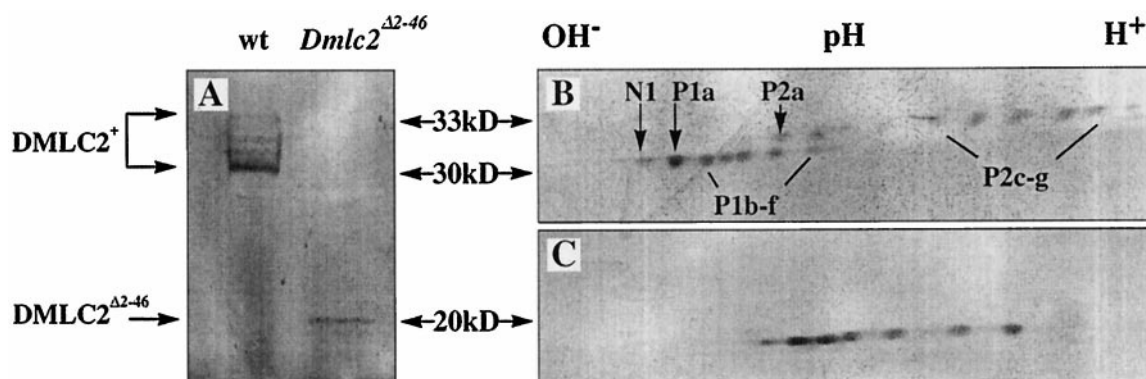

FIGURE 2 Western blot analysis of DMLC2 from mutant and wild-type lines. (*A*) One-dimensional Western blot of proteins extracted from mutant and wild-type thoraces. *Lane 1*: Wild type. *Lane 2*: $Dmlc2^{\Delta 2-46}$ homozygotes. In this gel system wild-type DMLC2 migrates as a 30–33-kDa doublet considerably more slowly than its calculated molecular mass would indicate. DMLC2$^{\Delta 2-46}$ migrates faster, at its calculated molecular mass of ~22 kDa. (*B*) Two-dimensional Western blot of wild-type DMLC2. Between 13 and 16 isoelectric variants that group into two broad molecular weight categories are detected. N1 corresponds to the nonphosphorylated isovariant. The other isovariants are phosphorylated. The P1 series corresponds to the ~30-kDa category, and the P2 series corresponds to the ~33-kDa category. (*C*) Two-dimensional Western blot of homozygous $Dmlc2^{\Delta 2-46}$ flies. Note that the truncated DMLC2 runs at a molecular mass that is lower than and has an isoelectric point that is different from those of wild-type DMLC2, as would be predicted by the removal of residues in the N-terminus. The polyclonal antibody recognizes approximately seven isovariants. In addition to demonstrating an altered isovariant pattern, these results show that no wild-type DMLC2 is expressed. All blots were probed with a polyclonal antibody to bacterially expressed DMLC2 (Dickinson et al., 1997).

Isovariants N1 and P1 correspond to the 30-kDa band and the P2 isovariants correspond to the 33-kDa band.

Analysis of proteins extracted from $Dmlc^{\Delta 2-46}$ flies shows the calculated shift in isoelectric point as well as the shift in molecular mass for N1 (Fig. 2 *C*). There were, however, significant changes in the isovariant profile of the $Dmlc2^{\Delta 2-46}$ mutant. A large reduction in molecular mass was observed as expected with the truncation, but the larger and most acidic isovariants found in wild-type DMLC2 were conspicuously absent. The absence of the higher molecular mass variants in $Dmlc2^{\Delta 2-46}$ flies suggests that modification of the N-terminus is responsible for generating several of the isovariants of DMLC2.

Dmlc2$^{\Delta 2-46}$ rescues the dominant flightless phenotype of Dmlc2^{E38} heterozygotes

Flies heterozygous for $Dmlc2^{E38}$ are flight impaired because of abnormal IFM ultrastructure (Warmke et al., 1992). To determine if the N-terminus of DMLC2 is required for flight, we compared the flight ability of flies expressing various combinations of mutant and wild-type $Dmlc2$ genes (Table 1). $Dmlc2^{E38}$ heterozygotes were flightless, as indicated by a flight index of 0.4 $\pm$ 0.7 compared to 5.6 $\pm$ 0.25 for wild type. This deficit is rescued by a single copy of $Dmlc2^+$ (Warmke et al., 1992). Surprisingly, introducing a single copy of the truncated form, $Dmlc2^{\Delta 2-46}$, also rescues the flight behavior phenotype (flight index = 5.5 $\pm$ 0.27) of heterozygous $Dmlc2^{E38}$ flies. The wing beat frequency of these flies was significantly elevated (220 $\pm$ 9 Hz) compared to wild type (197 $\pm$ 5 Hz; p = 0.04) but was still within the normal range. The normal flight ability of the transheterozygous $Dmlc2^{\Delta 2-46}/Dmlc2^+$ flies implies that the ultrastructural defect of the $Dmlc2^{E38}$ mutation is rescued by a single copy of $Dmlc2^{\Delta 2-46}$. Because the $Dmlc2^{\Delta 2-46}$ gene lacks the N-terminus of DMLC2, these results suggest that either the N-terminus has no role in sarcomeric structure or ~50% of DMLC2 lacking the N-terminus along with ~50% of wild-type DMLC2 is suffi-

cient to permit the functional assembly of the muscle. To differentiate these two possibilities we studied homozygous $Dmlc2^{\Delta 2-46}$ flies.

Homozygous Dmlc2$^{\Delta 2-46}$ flies have normal IFM ultrastructure and are flight competent

The $Dmlc2^{E38}$ null mutation is recessive lethal (Warmke et al., 1992), and flies homozygous for this mutation die as embryos. The lethality is rescued by transformation with a wild-type $Dmlc2$ gene (Warmke et al., 1992). Although one copy of $Dmlc2^{\Delta 2-46}$ rescues the recessive lethality of the $Dmlc2^{E38}$ homozygotes, these flies are flightless (Table 1), as are flies hemizygous for the wild-type $Dmlc2$ (Table 1).

To determine if the N-terminus of DMLC2 is required for normal myofibrillogenesis, we compared the ultrastructure of intact IFM from flies homozygous for $Dmlc2^{\Delta 2-46}$ and of wild-type flies. Longitudinal sections of IFM from mutant flies are indistinguishable from wild type (Fig. 3 *A*). Myofibrils run the full length of the muscle fiber and exhibit well-defined sarcomeres with characteristically short I bands. Cross sections of mutant IFM show cylindrically shaped myofibrils surrounded by numerous mitochondria (Fig. 3 *B*). Myofibrils show the typical double hexagonal packing of thick and thin filaments found in wild-type IFM. These results show that removal of the N-terminal extension of DMLC2 has no obvious effect on myofibrillar structure at the level of the sarcomere (>50 nm). IFM are particularly sensitive to $Dmlc2^+$ dosage; therefore the normal ultrastructure also suggests that the transformed genes are expressed at levels near those of wild type (Warmke et al., 1992; Bernstein et al., 1993).

Because the sarcomeric structure of IFM from flies homozygous for $Dmlc2^{\Delta 2-46}$ was normal, any effect of the N-terminal truncation on flight performance and wing beat frequency can be attributed specifically to the loss of the N-terminus of DMLC2 and not to gross ultrastructural abnormalities. The flight index and wing beat frequency of flies homozygous for $Dmlc2^{\Delta 2-46}$ were not statistically different from the values for wild type (Table 1).

Flight kinematics of DMLC2$^{\Delta 2-46}$ flies

Although the flight box performance of $Dmlc2^{\Delta 2-46}$ homozygotes was comparable to that of wild type, the animals often displayed a peculiar trajectory at the onset of flight. Unlike wild-type flies that fly up toward the light source, mutant flies typically either hovered or momentarily dropped before flying upward. Because the flight box cannot quantify this difference we employed a more sensitive in vivo analysis, using a visual closed-loop flight arena (Lehmann and Dickinson, 1997; Dickinson et al., 1997). While actively fixating the position of a vertical stripe, the flies were induced to modulate flight performance by vertical
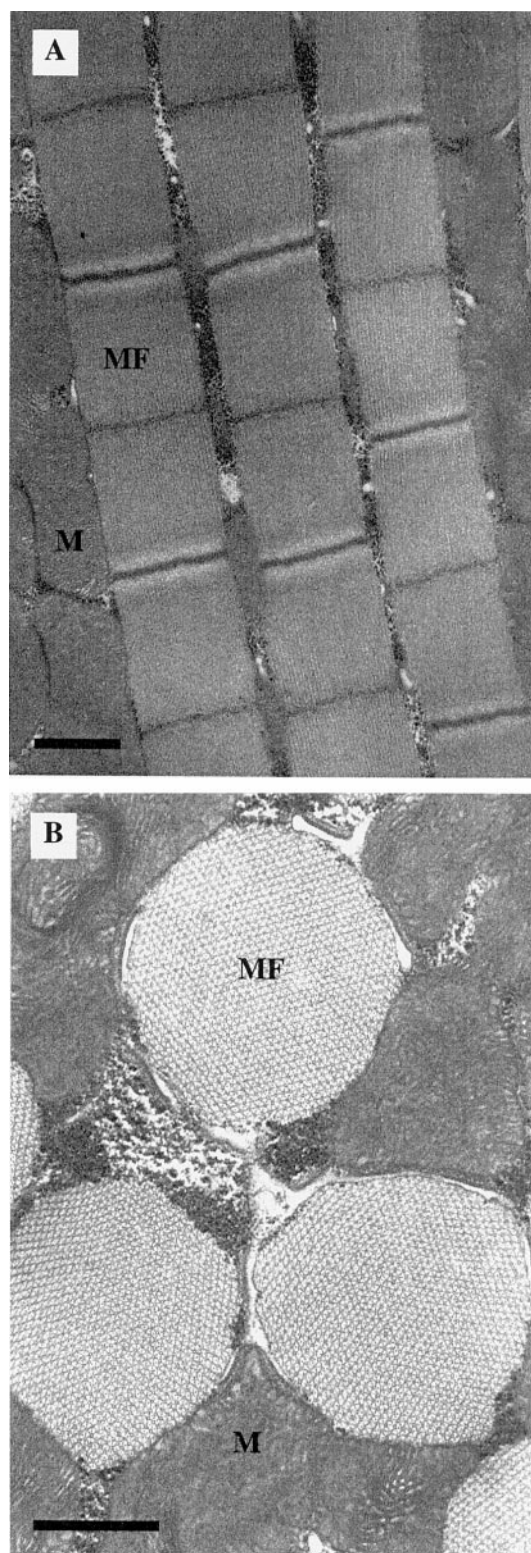
TABLE 1   Rescue of flightless behavior and recessive lethality of $Dmlc2^{E38}$

Genotype	Copy no. $Dmlc2^+$	Copy no. $Dmlc^{\Delta 2-46}$	Flight index (0–6)	Wbf (Hz)
E38/E38	0	0	*	*
E38/+	1	0	0.37 ± 0.13	137 ± 10
Δ2-46/E38	0	1	0.64 ± 0.19	ND
Δ2-46/+	1	1	5.5 ± 0.27	220 ± 9
Δ2-46/Δ2-46	0	2	5.2 ± 0.27	187 ± 15
+/+	2	0	5.6 ± 0.05	197 ± 5

*E38/E38 is embryonic lethal.
ND, not determined.
Flight indices were calculated and wing beat frequencies measured for each genotype (see Materials and Methods). The copy number refers to whether the particular line is haploid or diploid for $Dmlc2^+$ or $Dmlc2^{\Delta 2-46}$.

FIGURE 3 IFM from $Dmlc2^{\Delta2-46}$ flies have normal ultrastructure. (*A*) Longitudinal section of mutant IFM showing well-defined sarcomeres (3.0 ± 0.01 μm). Note the characteristically short I bands and well-defined A-bands (bar = 2 μm). Mutant ultrastructure is similar to that of the wild type. (B) Transverse sections of mutant IFM showing several myofibrils (MF). Note the ordered circular myofibrils and numerous mitochondria (M) characteristic of wild-type IFM (bar = 1 μm).

oscillation of a superimposed pattern of horizontal stripes. The results of the flight arena experiments are presented in Table 2 and represent the values collected when flies produced flight force levels that were within 1% of their maximum. $Dmlc2^{\Delta2-46}$ flies showed a 35% reduction in peak flight performance compared to wild type, as measured by the ratio of maximum flight force to body weight. This reduction correlates with a 31% drop in peak total metabolic rate ($P^*_{CO_2}$). Mechanical power (P^*_{mech}), calculated from stroke kinematics and morphometric parameters, was also reduced in mutant flies, although muscle efficiency ($P^*_{mech}/P^*_{CO_2}$) was not statistically different from wild-type values. The reduction in P^*_{mech} was due to a 7% drop in wing beat amplitude and a 5% drop in stroke frequency during peak force production. Mechanical power is expected to have a roughly cubic dependence on these two kinematic parameters (Dickinson et al., 1997). Although the mutant clearly displayed deficits in flight performance, they were nevertheless capable of generating flight force comparable to body weight and mechanical power in excess of 40 W kg^{-1}. Thus the IFM in flies possessing a truncated form of DLMC2, though compromised, remains functional.

Mechanical analysis of skinned IFM fibers

Previous studies (Morano et al., 1995) have shown that the addition of a synthetic peptide corresponding to residues 5–14 of MLC1 increases maximum and submaximum isometric force production. In *Drosophila* IFM steady-state tension began to rise at pCa 7 and reached a maximum at pCa 5 for both mutant and wild-type strains (Table 3). DMLC2 truncation had no significant effect on either maximum (wild type: 2.1 ± 1.1 kN/m^2; $Dmlc2^{\Delta2-46}$: 1.3 ± 0.55 kN/m^2; means ± SD) or submaximum (pCa 6) isometric tension (wild type: 1.0 ± 0.7 kN/m^2; $Dmlc2^{\Delta2-46}$: 0.8 ± 0.6 kN/m^2; means ± SD; Table 3).

After reaching steady-state isometric tension at various levels of calcium activation, skinned IFM fibers were oscillated lengthwise over a range of sinusoidal frequencies from 0.5 to 1000 Hz. The changes in dynamic stiffness and phase produced by the fibers in response to the length perturbations were analyzed graphically using Bode plots (Fig. 4). In maximally calcium-activated IFM, Bode plots have a characteristic triphasic shape that results from pronounced phase shifts in the intermediate frequency range. The plot of phase versus frequency (Fig. 4 *A*) shows no significant differences between IFM from mutant flies and that from wild type, suggesting similar contraction kinetics. The plot of $Dmlc2^{\Delta2-46}$ IFM dynamic stiffness versus frequency (Fig. 4 *B*) shows a form similar to that of wild-type IFM, although the stiffness amplitude was reduced.

Dynamic stiffness can be separated into in-phase and out-of-phase components, which represent the elastic (E_e) and viscous (E_v) moduli, respectively. The reduction in dynamic stiffness could result from a reduction in E_v and/or

TABLE 2   Flight kinematics during peak conditions

	Force/weight	Wbf (Hz)	Amplitude (degrees)	P_{CO_2} (W/kg)	Efficiency (%)	P_{mech} (W/kg)
Wild type*	1.35 ± 0.18	207 ± 1	170 ± 3	695 ± 103	9.7 ± 1.1	80 ± 13
$\Delta2\text{-}46/\Delta2\text{-}46$[†]	0.98 ± 0.28[‡]	196 ± 2	158 ± 6[§]	479 ± 95[§]	8.6 ± 1.1	42 ± 13[§]

Values are means $\pm$ SD for maximum flight performance, as indicated in Materials and Methods (*$n = 7$, [†]$n = 10$, [‡]$p < 0.01$, [§]$p < 0.001$). Flight force/weight, the ratio of maximum active force to body weight; P_{CO_2}, CO_2 output of active flies during flight corrected for CO_2 output at rest. P_{mech}, mechanical power output calculated from flight force and morphometric parameters; Efficiency, the ratio of total power output to aerodynamic power output (Dickinson and Lighton, 1995).

E_e in mutant IFM. Fig. 5 *A* shows that the reduction in mutant IFM dynamic stiffness results primarily from a reduction in E_e, the magnitude of which represents the elastic properties of the muscle. E_v, on the other hand, is a property of the active interaction of actin and myosin, and its magnitude provides a direct measure of the work absorbed or generated by the muscle during cyclic oscillation. As indicated in Fig. 5 *B*, the magnitude of E_v is not significantly affected by N-terminal truncation of DMLC2 (Fig. 5 *B*). Power (P^*_{IFM}) output was not significantly different in mutant and wild-type flies ($p = 0.18$). Likewise, the frequency at which maximum power was achieved was unchanged in the transformed line (Table 4) ($p = 0.44$).

DISCUSSION

DMLC2 has been shown to play a role in both myofibrillogenesis (Warmke et al., 1992) and the regulation of stretch activation (Tohtong et al., 1995). The molecular-genetic and integrative biophysical studies possible with the fruit fly (Maughan and Vigoreaux, 1999) make it an excellent experimental organism for identifying the DMLC2 domains that are required for these respective functions. Here we use a "reverse genetic" approach to show that the unique 46-amino acid N-terminal extension of DMLC2 plays little or no role in myofibrillogenesis and has little effect on the work producing properties of the myosin cross-bridge in isolated skinned IFM. However, removal of the extension does affect flight performance, possibly by reducing the IFM in-phase stiffness. One interpretation of these results is that the DMLC2 N-terminal extension functions as a passive link in parallel with the cross-bridges.

Altered isovariant profile in DMLC2$^{\Delta2-46}$ flies

Analysis of proteins extracted from wild-type flies by 2D SDS-PAGE reveals numerous isovariants of DMLC2 (Mogami et al., 1982; Takano-Ohmuro et al., 1990; Dickinson et al., 1997). Although earlier studies identified only three isoelectric variants, spots 138, 148, and 149 (Mogami et al., 1982), 2D gels with a more shallow pH gradient demonstrate that the major spots defined by Mogami et al. (1982) consist of multiple isoelectric variants each, for a total of ~14 (Dickinson et al., 1997). The most acidic 13 isovariants are phosphorylated (Takano-Ohmuro et al., 1990; Dickinson et al., 1997).

Phosphorylation of vertebrate MLC2 by MLCK has been shown to regulate smooth muscle contraction (Trybus,
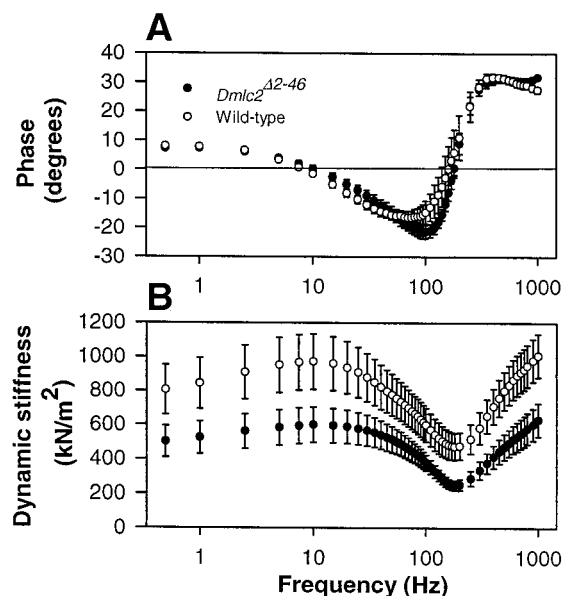

FIGURE 4 Phase shift and complex stiffness modulus of maximally Ca^{2+}-activated mutant IFM fibers compared to wild type. (*A*) Phase shift as a function of frequency for wild type ($\bigcirc$) and mutant ($\bullet$). Note that phase inversion occurs at the same frequency in mutant IFM. (*B*) The complex stiffness modulus of wild-type ($\bigcirc$) and *Dmlc2*$^{\Delta2-46}$ ($\bullet$) as a function of frequency. The stiffness minimum occurs at a frequency that is approximately equal to the frequency of phase inversion. The stiffness modulus is decreased for the mutant compared to wild type. Note that the stiffness minimum is achieved at a frequency similar to that of the wild type.
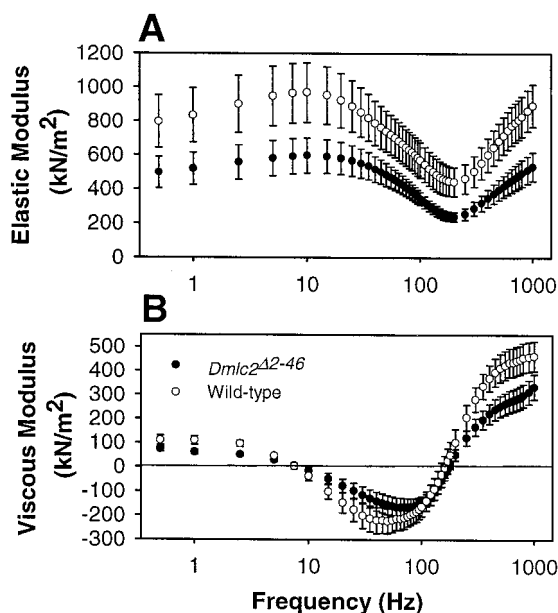
TABLE 3   Isometric force and oscillatory power at both maximum and submaximum conditions

pCa	7	6	5.5	5
Wild type*	0.08 ± 0.04	0.42 ± 0.11	0.96 ± 0.02	1
$\Delta2\text{-}46/\Delta2\text{-}46$[†]	0.03 ± 0.03	0.56 ± 0.14	0.99 ± 0.02	1

Normalized isometric force values are expressed as means $\pm$ SEM (*$n = 7$ for wild type and [†]$n = 9$ for mutant) for various levels of calcium activation ranging from pCa8 to pCa5. There is no significant difference between mutant and wild-type IFM.

FIGURE 5 Elastic and viscous moduli of maximally Ca^{2+}-activated mutant and wild-type IFM. (*A*) Elastic moduli for mutant and wild-type IFM as a function of frequency. The elastic modulus is decreased for the mutant compared to wild type, indicating that the reduction in $Dmlc2^{\Delta2-46}$ dynamic stiffness is due primarily to a reduction in the elastic modulus. (*B*) Viscous moduli for mutant and wild-type IFM. Points above zero correspond to a phase lead of the tension with respect to length at the frequency indicated (i.e., work is done on the muscle by the apparatus). Points below zero correspond to a phase lag (the muscle does work on the apparatus). Note that there is no significant difference in viscous moduli near the frequency of maximum power output (see also Table 4) between mutant and wild type, indicating a similar ability to produce oscillatory work.

1994). In striated muscle contraction, phosphorylation appears to have only a modulatory role (Sweeney et al., 1993). Phosphorylation of skeletal muscle MLC2 increases the submaximum isometric tension (Persechini *et al.,* 1985) and the rate of force development (Metzger et al., 1989). One mechanism proposed to explain the effects on force production in striated muscle is that phosphorylation causes myosin heads to move away from the thick filament backbone toward the thin filament, thus increasing the probability of actomyosin interactions.

DMLC2 has been shown to be phosphorylated by MLCK (Takano-Ohmuro et al., 1990). Substitution of the MLCK substrate serines for alanines resulted in a marked reduction in oscillatory work and power production in *Drosophila* IFM, as well as a slightly altered isovariant profile (Dickinson et al., 1997). The subtle reduction in phosphovariants suggested that many of the phosphovariants result from phosphorylation by protein kinases other than MLCK.

Analysis of proteins extracted from homozygous $Dmlc2^{\Delta2-46}$ flies by 2D SDS-PAGE revealed a pattern lacking several of the isovariants observed in wild-type flies. The region of the N-terminus between amino acids 2 and 46 of DMLC2 contains five serines and six threonines. Some of these are potential substrates for known protein kinases (for example, T13 is in a consensus sequence for cyclic AMP-dependent kinase and casein kinase). The reduction in the number of spots suggests that some of the residues in the N-terminus of wild-type DMLC2 are phosphorylated. Alternatively, removing residues 2–46 could affect kinase recognition and, presumably, phosphorylation at residues outside the N-terminus.

There are two forms of essential light chain in vertebrate skeletal muscle, MLC1 and MLC3. MLC1 differs from MLC3 by the addition of 41 residues at the N-terminus that are not found in the otherwise homologous MLC3 (Collins, 1991). The N-terminus of MLC1 is characterized by a cluster of basic residues that is separated from the rest of the molecule by a proline-alanine-rich region, a motif that is similar to that of the DMLC2 N-terminal extension. Like DMLC2, vertebrate skeletal and cardiac muscle MLC1 also show abnormally slow migration in SDS-PAGE. Given that removal of the DMLC2 N-terminus causes DMLC2$^{\Delta2-46}$ to migrate at its true molecular mass, it is possible that the proline-alanine sequences in the extension result in the retarded gel mobility of both MLC1 and DMLC2.

DMLC2$^+$ N-terminal truncation has no discernible effect on IFM sarcomeric structure

The myofilament lattice of *Drosophila* IFM consists of an ordered double-hexagonal array of thick and thin filaments. Myofilaments in the periphery of the DMLC2 null

TABLE 4 Summary of isolated IFM dynamic stiffness data

	F_{max} (Hz)	E_e (kN/m^2)	E_v (kN/m^2)	$P_{oscillatory}$ (W/m^3)	Dynamic stiffness (kN/m^2)
Wild-type*	102 ± 14	580 ± 106	196 ± 32	112 ± 37	614 ± 109
Δ2-46/Δ2-46[†]	112 ± 5	334 ± 43[‡]	154 ± 33	67 ± 11	371 ± 52[‡]

Averaged sinusoidal analysis data from wild-type and mutant IFM at the frequency at which power is maximum. Values are means and SEM for *$n = 7$, [†]$n = 11$, [‡]$p < 0.05$. E_e refers to the elastic modulus (in phase) stiffness. E_v refers to the viscous (out of phase) stiffness. Dynamic stiffness is the vector sum of E_e and E_v. Power output (W/m^3) was calculated from the viscous modulus, the amplitude and frequency of the length change, and the fiber cross-sectional area and length, using the formula Power = $\pi f E_v ([\Delta L/L]_{rms})^2$, where f is frequency (Hz), E_v is the viscous modulus (kN/m^2), ΔL is half the peak-to-peak amplitude of the applied sinusoidal length change, L is the length of the muscle fiber, and rms is the root mean square of the applied length perturbation. Temperature, 12°C.

($Dmlc2^{E38}$) heterozygote myofibrils are grossly disorganized, demonstrating that two copies of the $Dmlc2^+$ gene are required for normal myofibrillogenesis and proper integration of thick and thin filaments (Warmke et al., 1992).

Assuming an extended structure, the proline-rich 46-amino acid DMLC2 N-terminus can span the 8-nm distance from the myosin S1 neck to the thin filament (Trayer et al., 1987; Williamson, 1994; Timson and Trayer, 1997). Results from NMR studies (Trayer et al., 1987), cross-linking studies (Sutoh, 1982), and electron microscopic reconstructions of actin decorated with S1 (Milligan et al., 1990) indicate that the MLC1 extension contacts actin. Furthermore, mutagenesis of the N-terminal lysines of MLC1 to alanines or glutamate in skeletal muscle fibers produces an increase in unloaded shortening velocity (Sweeney, 1995), suggesting that the interaction of the basic N-terminus of MLC1 with actin could act as a tether that slows actomyosin kinetics. Because of its similarity to the MLC1 N-terminus, it is possible that the DMLC2 N-terminus also contacts actin and that the resulting interaction plays a role in myofilament alignment.

Analysis of electron micrographs of IFM from $Dmlc2^{\Delta2-46}$ flies shows that, despite its putative interaction with actin, removal of the N-terminal extension has no obvious effect on sarcomeric structure, suggesting that any interaction of the N-terminus of DMLC2 with actin has little effect on the assembly and stability of the myofilament lattice in IFM. The normal structure allows us to attribute any phenotypic difference of mutant flies directly to the loss of the N-terminus and not to gross sarcomeric structural alterations. In addition, the normal structure suggests that mutant protein expression levels are near that of wild-type.

Flight ability of Dmlc2$^{\Delta2-46}$ flies

Although $Dmlc2^{\Delta2-46}$ flies can fly, they exhibit altered behavior at the onset of flight, which suggests a partial impairment of their force-generating capability. More sensitive flight arena measurements directly quantified the effects of N-terminal truncation of DMLC2. The truncation resulted in a 35% reduction in the flight force-weight ratio compared to wild type (Table 2), a 47% decrease in mechanical power, and a 31% decrease in maximum metabolic power output. Because ~90% of metabolic output during flight can be attributed to the activity of the flight muscles (Lehmann and Dickinson, 1997), the decrease represents a reduction in the work generated by the IFMs. The drop in mechanical power output (P^*_{mech}) in mutant flies, estimated from kinematics measurements in the flight arena, was roughly equivalent to the reduction in total metabolic power, which indicates that the mechanical efficiencies of mutant and wild-type muscle are comparable. Furthermore, although the power-generating capability appears to be reduced because of truncation of the N-terminal extension of DMLC2, the mutant muscle is still capable of generating

over 40 W kg^{-1}, a value that is still large compared to most locomotory muscles (Josephson, 1993) and just large enough to support flight. The attenuated mechanical power output (P^*_{mech}) correlates with a drop in maximum wing beat amplitude and stroke frequency, which are determined in part by the resonant properties of the thoracic muscular-cuticle system, as well as the function of control muscles (Dickinson and Tu, 1998). One possible explanation for the diminished performance is an unfavorable shift in resonance caused by the altered elastic properties identified in the skinned-fiber experiments.

DMLC2$^{\Delta2-46}$ skinned fiber mechanics

The oscillatory movement of IFM is powered by stretch activation, a phenomenon exhibited by all striated muscles, where tension rises as a delayed response to stretch from the isometric state. Stretch activation is particularly prominent in IFM (Pringle, 1978) and cardiac muscle (Steiger, 1977). Its high amplitude provides the power for flight in insects (Pringle, 1978) and has been suggested to function in papillary muscle (Poetter et al., 1996; Vemuri et al., 1999). Several models have been proposed to explain the enhanced stretch activation response of insect IFM (Thorson and White, 1983; Granzier and Wang, 1993; Tohtong et al., 1995). One model involves the interaction of the unique N-terminal extension of DMLC2 with the thin filament (Tohtong et al., 1995). In this model, DMLC2 acts as a tether, which promotes actomyosin interactions leading to enhanced stretch activation. The relatively normal oscillatory work in $Dmlc2^{\Delta2-46}$ IFM as indicated by the viscous modulus (E_v) (Table 4) suggests that the DMLC2 extension plays only a minor role in the stretch activation response of *Drosophila* IFM.

Incubation of skinned atrial muscle fibers with a peptide corresponding to amino acids 4–13 of human ventricular MLC1 increases both submaximum isometric force production and the rate of force development (Morano et al., 1995). The same peptide also induced an increase in myofibrillar ATPase at submaximum calcium levels (Rarick et al., 1996). Surprisingly, we found that the removal of the N-terminal extension of DMLC2 has no significant effect on submaximum or maximum isometric tension (Table 3). Other studies of cardiac muscle MLC1 have shown more subtle effects on the calcium sensitivity of isometric tension, depending on the amount of atrial MLC1 isoform present in skinned ventricular strips (Schaub et al., 1998). Therefore, it is possible that removal of the DMLC2 N-terminal extension has less obvious effects than those investigated here.

Osmotic compression studies on skinned (Millman, 1998, and references therein) and intact (Checci and Bagni, 1994) muscle fibers indicate that the force-generating mechanism of the myosin cross-bridge is affected by lattice spacing change. Preliminary x-ray diffraction measurements (Bhattacharya, Irving, and Maughan, unpublished observations)

indicate that the filament lattice of *Drosophila* IFM is swollen by at least 2% after skinning. Thus it is possible that fiber swelling masks any effects of DMLC2 truncation, particularly if the effect is subtle. Assessment of this possibility awaits future studies in which mutant and wild-type fibers are compressed osmotically back to their in vivo myofilament spacing.

The role of DMLC2$^+$

The sarcomeric structure of insect indirect flight muscles is similar to that of other striated (skeletal) muscles. However, several structural and physiological modifications have presumably evolved to provide the high power requirements of flight. One of these modifications is a characteristically high passive stiffness. Passive stiffness is important to the insect flight system because the downstroke kinetic energy is stored in the dorsal ventral indirect flight muscles for use during the upstroke. Comparably, the force produced by the upstroke muscles must be stored within the dorsal longitudinal indirect flight muscles, where it can be used to generate the downstroke (Dickinson and Lighton, 1995). As the two muscle groups contract alternately, they feed a resonant system consisting of the wings, thorax, and the muscles themselves. Altered stiffness of the flight muscles would cause both a reduction in elastic storage and an unfavorable shift in the resonant frequency of the flight system, which would lead to the observed flight impairment.

The indirect flight muscles of *Drosophila melanogaster* possess several unique or modified versions of the usual contractile proteins. Some of these proteins, TnH (Reedy et al., 1994) and DMLC2 (Tohtong et al., 1995), have been proposed to form cross-links between the thick and thin filaments. Such lateral interactions between filaments could generate significant longitudinal force when the muscle is stretched.

IFM from *Dmlc2*$^{\Delta 2-46}$ flies exhibits a small but significant reduction in the elastic modulus (E_e), which correlates with a demonstrable attenuation of flight performance. The reduction in E_e without a reduction in the viscous modulus (E_v) is consistent with the N-terminal extension being a parallel link between the thick and thin filaments, which contributes to passive stiffness but has only minor effects on the power-producing properties of the myosin cross-bridge.

REFERENCES

Anson, M., D. R. Drummond, M. A. Geeves, E. S. Hennessey, M. D. Ritchie, and J. C. Sparrow. 1995. Actomyosin kinetics and in vitro motility of wild-type *Drosophila* actin and the effects of two mutations in the *Act88F* gene. *Biophys. J.* 68:1991–2003.

Bernstein, S. I., P. T. O'Donnell, and R. M. Cripps. 1993. Molecular genetic analysis of muscle development, structure, and function in *Drosophila. Int. Rev. Cytol.* 143:63–152.

Checci, G., and M. Bagni. 1994. Myofilament lattice spacing affects tension in striated muscle. *News Physiol. Sci.* 9:3–7.

Collins, J. H. 1991. Myosin light chains and troponin C: structural and evolutionary relationships revealed by amino acid sequence comparisons. *J. Muscle Res. Cell Motil.* 12:3–25.

Dickinson, M. H., C. J. Hyatt, F. Lehmann, J. R. Moore, M. C. Reedy, A. Simcox, R. Tohtong, J. O. Vigoreaux, H. Yamashita, and D. W. Maughan. 1997. Phosphorylation-dependent power output of transgenic flies: an integrated study. *Biophys. J.* 73:3122–3134.

Dickinson, M. H., and J. R. B. Lighton. 1995. Muscle efficiency and elastic storage in the flight motor of *Drosophila melanogaster. Science.* 128:87–89.

Dickinson, M. H., and Tu. 1998. The function of *Dipteran* flight muscle. *Comp. Biochem. Physiol.* 116A:223–238.

Drummond, D. R., M. Peckham, J. C. Sparrow, and D. C. S. White. 1990. Alteration in cross-bridge kinetics caused by mutations in actin. *Nature.* 348:440–442.

Granzier, H. L. M., and K. Wang. 1993. Interplay between passive tension and strong and weak binding cross-bridges in insect indirect flight muscle: a functional dissection by gelsolin-mediated thin filament removal. *J. Gen. Physiol.* 101:235–270.

Hill, T. L., E. Eisenberg, and L. Greene. 1980. Theoretical model for the cooperative equilibrium binding of myosin subfragment 1 to the actin-troponin-tropomyosin complex. *Proc. Natl. Acad. Sci. USA.* 77:3186–3190.

Hyatt, C. J., and D. W. Maughan. 1994. Fourier analysis of wing beat signals: assessing the effects of genetic alterations of flight muscle structure in *Diptera. Biophys. J.* 67:1149–1154.

Josephson, R. K. 1993. Contraction dynamics and power output of skeletal muscle. *Annu. Rev. Physiol.* 55:527–546

Lehmann, F.-O., and M. H. Dickinson. 1997. The changes in power requirements and muscle efficiency during elevated force production in the fruit fly, *Drosophila melanogaster. J. Exp. Biol.* 200:1133–1143.

Metzger, J. M., M. L. Greaser, and R. L. Moss. 1989. Variations in cross-bridge attachment rate and tension with phosphorylation of myosin in mammalian skinned skeletal muscle fibers: implications for twitch potentiation in intact muscle. *J. Gen. Physiol.* 93:855–883.

Milligan, R. A., M. Whittaker, and D. Safer. 1990. Molecular structure of F-actin and location of surface binding sites. *Nature.* 348:217–221.

Millman, B. M. 1998. The filament lattice of striated muscle. *Physiol. Rev.* 78:359–391.

Maughan, D. W., and J. O. Vigoreaux. 1999. An integrated view of insect flight muscle: genes, motor molecules and motion. *News Physiol. Sci.* 14:87–92.

Mogami, K., S. C. Fugita, and Y. Hotta. 1982. Identification of *Drosophila* indirect flight muscle myofibrillar proteins by means of two-dimensional electrophoresis. *J. Biochem.* 91:643–650.

Morano, I., O. Ritter, A. Bonz, T. Timek, C. F. Vahl, and G. Michel. 1995. Myosin light chain-actin interaction regulates cardiac contractility. *Circ. Res.* 76:720–725.

Morano, M., U. Zacharzowski, M. Maier, P. E. Lange, V. Alexi-Meskishvili, and H. Haase. 1996. Regulation of human heart contractility by essential myosin light chain isoforms. *J. Clin. Invest.* 98:467–473.

Parker, V. P., S. Falkenthal, and N. Davidson. 1985. Characterization of the myosin light-chain-2 gene of *Drosophila melanogaster. Mol. Cell. Biol.* 5:3058–3068.

Persechini, A., J. T. Stull, and R. Cooke. 1985. The effect of myosin phosphorylation on the contractile properties of skinned rabbit skeletal muscle fibers. *J. Biol. Chem.* 260:7951–7954.

Pirrotta, V. 1988. Vectors for P-mediated transformation in Drosophila. *Biotechnology.* 10:437–456.

Poetter, K., H. Jiang, S. Hassanzadeh, S. R. Master, A. Chang, M. C. Dalakas, I. Rayment, J. R. Sellers, L. Fananapazir, and N. D. Epstein.

1996. Mutations in either the essential or regulatory light chains of myosin are associated with a rare myopathy in human heart and skeletal muscle. *Nature Genet.* 13:63–69.

Pringle, J. W. S. 1978. The Croonian Lecture, 1977. Stretch activation of muscle; function and mechanism. *Proc. R. Soc. Lond. B.* 201:107–130.

Rarick, H. M., T. J. Opgenorth, T. W. von Geldern, J. R. Wu-Wong, and R. J. Solaro. 1996. An essential myosin light chain peptide induces supramaximal stimulation of cardiac myofibrillar ATPase activity. *J. Biol. Chem.* 271:27039–27043.

Reedy, M. C., M. K. Reedy, K. R. Leonard, and B. Bullard. 1994. Gold/Fab immuno electron microscopy localization of troponin H and troponin T in *Lethocerus* flight muscle. *J. Mol. Biol.* 239:52–67.

Rubin, G. M., and A. C. Spradling. 1982. Genetic transformation of Drosophila with transposable element vectors. *Science.* 218:348–353.

Schaub, M. C., M. A. Hefti, R. A. Zuellig, and I. Morano. 1998. Modulation of contractility in human cardiac hypertrophy by myosin essential light chain isoforms. *Cardiovasc. Res.* 37:381–404.

Steiger, G. J. 1977. Stretch activation and tension transients in cardiac, skeletal and insect flight muscle. *In* Insect Flight Muscle. R. T. Tregear, editor. Elsevier North Holland Biomedical Press, Amsterdam. 221–268.

Sutoh, K. 1982. Identification of myosin binding sites on the actin sequence. *Am. Chem. Soc.* 21:3654–3661.

Sweeney, H. L. 1995. Function of the N terminus of the myosin essential light chain of vertebrate striated muscle. *Biophys. J.* 68:112s–119s.

Sweeney, H. L., B. F. Bowman, and J. T. Stull. 1993. Myosin light chain phosphorylation in vertebrate striated muscle: regulation and function. *Am. J. Physiol.* 264:C1085–C1095.

Takano-Ohmuro, H., S. Takahashi, G. Hirose, and K. Maruyama. 1990. Phosphorylated and dephosphorylated myosin light chains of *Drosophila* fly and larva. *Comp. Biochem. Physiol.* 95B:171–177.

Thorson, J., and D. C. S. White. 1983. Role of cross-bridge distortion in the small-signal mechanical dynamics of insect and rabbit striated muscle. *J. Physiol. (Lond.).* 343:59–84.

Timson, D. J., and I. P. Trayer. 1997. The role of the proline-rich region in A1-type myosin essential light chains: implications for information transmission in the actomyosin complex. *FEBS Lett.* 400:31–36.

Toffenetti, J., D. Mischke, and M. L. Pardue. 1987. Isolation and characterization of the gene for myosin light chain two of *Drosophila melanogaster. J. Cell Biol.* 104:19–28.

Tohtong, R., H. Yamashita, M. Graham, J. Haeberle, A. Simcox, and D. Maughan. 1995. Impairment of muscle function caused by mutations of phosphorylation sites in myosin regulatory light chain. *Nature.* 374: 650–653.

Trayer, I. P., H. R. Trayer, and B. A. Levine. 1987. Evidence that the N-terminal region of A1-light chain of myosin interacts directly with the C-terminal region of actin: a proton magnetic resonance study. *Eur. J. Biochem.* 164:259–266.

Trybus, K. M. 1994. Role of myosin light chains. *J. Muscle Res. Cell Motil.* 15:587–594.

Vemuri, R., E. B. Lankford, K. Poetter, S. Hassanzadeh, K. Takeda, Z. X. Yu, V. J. Ferrans, and N. D. Epstein. 1999. The stretch-activation response may be critical to the proper functioning of the mammalian heart. *Proc. Natl. Acad. Sci. USA.* 96:1048–1053.

Warmke, J., M. Yamakawa, J. E. Molloy, S. Falkenthal, and D. W. Maughan. 1992. A myosin light chain-2 mutation affects flight, wing beat frequency and indirect flight muscle contraction kinetics in *Drosophila. J. Cell Biol.* 119:1523–1536.

Williamson, M. P. 1994. The structure and function of proline-rich regions in proteins. *Biochem. J.* 297:249–260.